

^{11}B NMR detection of the magnetic field distribution in the mixed superconducting state of MgB_2 .

G. Papavassiliou, M. Pissas, M. Fardis, M. Karayanni, and C. Christides*

Institute of Materials Science, National Center for Scientific Research "Demokritos", 153 10 Athens, Greece

(November 1, 2018)

The temperature dependence of the magnetic field distribution in the mixed superconducting phase of randomly oriented MgB_2 powder was probed by ^{11}B NMR spectroscopy. Below the temperature of the second critical (B_{c2}) field, $T_{c2} \approx 27\text{K}$, our spectra reveal two NMR signal components, one mapping the magnetic field distribution in the mixed superconducting state and the other one arising from the normal state. The complementary use of bulk magnetization and NMR measurements reveals that MgB_2 is an anisotropic superconductor with a $B_{c2}^c < 2.35$ Tesla anisotropy parameter $\gamma \approx 6$.

The recent discovery of superconductivity [1] in MgB_2 has revived the excitement on this area of research because this alloy becomes superconducting at unexpectedly [2] high temperatures ($T_c = 39\text{K}$), for "light" main group elements residing between Be and S in the periodic table. Subsequent studies have shown that MgB_2 is a type-II superconductor with $B_{c1}(0) \approx 0.26$ Tesla, $B_{c2}(0) \approx 14$ Tesla, with a small condensation energy (relative to Nb_3Sn and $\text{YBa}_2\text{Cu}_3\text{O}_7$), a $\xi_0 \approx 4.9$ nm, and a $\lambda_0 \approx 185$ nm [3]. However, opinions about the nature of the superconductivity mechanism are still contradictory. Band structure calculations [4] suggest that MgB_2 is a BCS superconductor, where superconductivity results from in-plane electron-phonon coupling on the boron sublattice. The detected isotope effect [5] and the BCS-type energy gap, that is obtained by tunneling spectroscopy [6] and ^{11}B NMR [7–9], are in support of this model. However, specific heat measurements indicate that the superconducting gap is either anisotropic or two-band-like [3]. Further deviations from the s -wave model have been detected on the temperature dependence of B_{c1} and λ [10] as well.

Recently few works [11–16] presented convincing evidence that the MgB_2 is an anisotropic superconductor with an anisotropy parameter $\gamma = (B_{c2}^{ab}/B_{c2}^c)$ taking values into interval $2 \leq \gamma \leq 6$.

In principle, a strong anisotropy in the mixed superconducting state of powder MgB_2 - if present- should be detectable with ^{11}B NMR spectroscopy. As known, for fields $B_{c1} < B_0 < B_{c2}$ a vortex lattice is formed that gives rise to a characteristic magnetic field distribution with van Hove singularities at fields where $\nabla \cdot B = 0$. For a perfect hexagonal vortex lattice the field distribution exhibits a peak at a value B_s , which corresponds to the saddle point located midway between two vortices, whereas two steps at the maximum (B_{max}) and minimum (B_{min}) fields are expected [17,18]. Such a magnetic field distribution should be mapped on the NMR line shape, as the Larmor frequency of the resonating nuclei

depends linearly on the local magnetic field. Successful mapping of the magnetic field distribution has been already presented in a variety of superconducting materials, like vanadium [17], and rare earth nickel borocarbides $\text{YNi}_2\text{B}_2\text{C}$ with ^{11}B NMR [19]. In case of strong anisotropy and in applied field $B_{c2}^c < B_0 < B_{c2}^{ab}$, a powder superconducting sample with randomly oriented grains is expected to give a superposition of magnetic field distributions, ranging in between the normal state and the Abrikosov lattice. It is thus of particular interest to testify the possibility of anisotropy in the mixed superconducting state of MgB_2 , by performing ^{11}B NMR experiments in magnetic fields fulfilling the above condition.

In this letter we report ^{11}B NMR line shape measurements on powder MgB_2 samples in external magnetic fields $B_0 = 2.35$ and 4.7 Tesla, which exhibit a strong asymmetric low frequency broadening at temperatures lower than the temperature of the second critical field ($T < T_{c2}$). The low temperature spectra may be decomposed in two components: One component corresponding to the unshifted NMR signal of the normal state, which indicates that a portion of the sample volume remains in the normal state even at the lowest measured temperature of 5K . A second component, which maps the magnetic field distribution of the vortex lattice in the mixed state (vortex component). Our data provide clear evidence that for a part of the MgB_2 grains the $B_{c2}(0) < 2.35$ Tesla, whereas for another part of the grains $B_{c2}(0)$ is sufficiently higher, and according to magnetic and CESR measurements [14] $B_{c2}^{ab}(0) \approx 14$ Tesla. Thus, our results provide a strong experimental evidence that MgB_2 is an anisotropic superconductor with an anisotropy parameter $\gamma \approx 6$.

High quality MgB_2 powder samples were prepared by liquid-vapor to solid reaction in an alumina crucible placed inside a vacuum sealed silica tube, using a 3% excess of Mg. Pure Mg and B powders were thoroughly mixed and subsequently slowly heated up to 910°C .

At this temperature the sample annealed for two hours and then cooled slowly down to room temperature. Rietveld refinement of x-ray powder diffraction spectra revealed that the examined sample consists of 95% MgB_2 , with cell constants equal to $a = b = 3.0849(1)$ Å and $c = 3.5213(1)$ Å, and a secondary phase of 5% MgO .

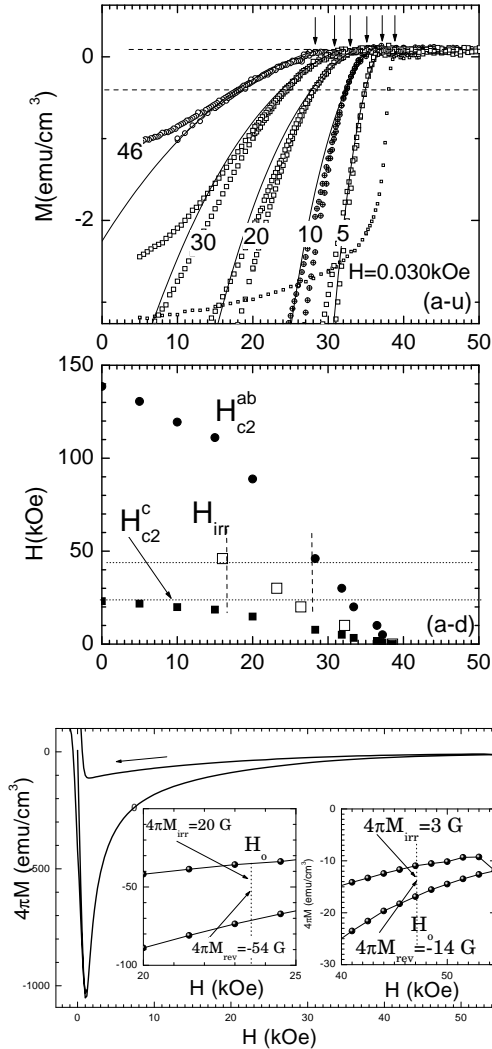


FIG. 1. (a) (upper panel) Zero field and field cooling magnetic moment as a function of the temperature for $H = 0.03, 5, 10, 20, 30$ and 46 kOe for the powder MgB_2 sample used in the NMR measurements. The line through the experimental points is a simulation of the reversible magnetic moment supposing an anisotropy $\gamma \approx 6$ (see main text). The lower panel shows the phase diagram where, the filled circles and squares correspond to H_{c2}^{ab} , H_{c2}^c lines respectively. The open squares represent the irreversibility line. (b) The half of the magnetization loop at $T = 5$ K. The insets show details in the region of $H = 2.35$ and $H = 4.7$ Tesla.

To investigate the mixed state and the magnetic irreversibility of MgB_2 we have employed thermomagnetic and isothermal magnetization measurements on a SQUID magnetometer. The upper panel of Figure 1a shows the

zero field (ZFC) and field cooling (FC) magnetization curves for a sample with randomly oriented grains, which was also used in the NMR measurements. A marked feature is the observed curvature near the onset of the transition, which has been recently attributed [14] to the anisotropy of MgB_2 . Specifically, the onset of the diamagnetic signal occurs at the B_{c2}^{ab} which varies with temperature as $B_{c2}^{ab}(T) = B_{c2}^{ab}(0)(1 - T/T_c)^{1.27}$. Since we examine a powder sample containing randomly oriented grains, we have applied the equation derived by Simon *et al* [14] for a uniaxial superconductor with the magnetization lying parallel to the external field, in order to fit the reversible part of the thermomagnetic curves. The solid line in Figure 1a shows the successful reproduction of the experimental data by using an anisotropy ratio $\gamma \sim 6$ and an average penetration depth: $\lambda = (\lambda_{ab}^2 \lambda_c)^{1/3} \approx 170$ nm, in agreement with the values in Ref. [14]. The lower panel of Figure 1a shows the phase diagram that is obtained from the magnetic measurements. This diagram includes the temperature variation of B_{c2}^c which is estimated from $B_{c2}^c = B_{c2}^{ab}/\gamma$. In this figure we also include the data of H_{c2}^{ab} for $H > 5.5$ T, from ref. [14]. The irreversibility line is derived from the temperature where the ZFC and the FC branches are separated. Finally, Figure 1b shows the half of the isothermal hysteresis loop at $T = 5$ K, which indicates that the irreversible magnetization is comparable to the reversible one. This small irreversible magnetization, in the powder sample has been attributed to the surface barriers [20]. The two insets show details of the loop in the regions of 2.35 and 4.7 Tesla, which are used below to reproduce the magnetic field distribution in the vortex lattice.

^{11}B NMR line shape measurements were performed on two spectrometers operating in external magnetic fields with $B_0 = 2.35$ and 4.7 Tesla. The spectra were obtained from the Fourier transformation of half of the echo, following a typical $\pi/2$ - τ - π spin-echo pulse sequence. In both magnetic fields and in the normal state the length of the $\pi/2$ pulse was $t_p(\pi/2) \leq 2 \mu\text{sec}$, corresponding to a radiofrequency (rf) irradiation field $B_1 \geq 44$ Gauss. At room temperature the spectra were found to exhibit the typical powder pattern for a nuclear spin $I = 3/2$ in the presence of quadrupolar effects with an axially symmetric electric field gradient, in agreement with previous works [8,21]. The separation of the symmetric satellite lines gives a quadrupolar frequency [22]: $\nu_Q = 2\Delta\nu^{(1)} = e^2qQ/2h \approx 0.836$ MHz. In Figure 2 we demonstrate the line shape of the central transition ($-\frac{1}{2} \rightarrow \frac{1}{2}$) as a function of temperature in a magnetic field of 4.7 Tesla. The line shape in the normal state is temperature independent and consistent with previous studies [8,9,21]. In addition, a second order quadrupolar split of ≈ 6 kHz is clearly observed. Considering that for $I = 3/2$ the second order quadrupolar split is given by [22]: $\Delta\nu^{(2)} = (25\nu_Q^2/144\nu_L)[I(I+1) - 3/4]$, we obtain a $\nu_Q \approx 0.860$ MHz, in agreement with the value obtained

from the separation of the satellite peaks.

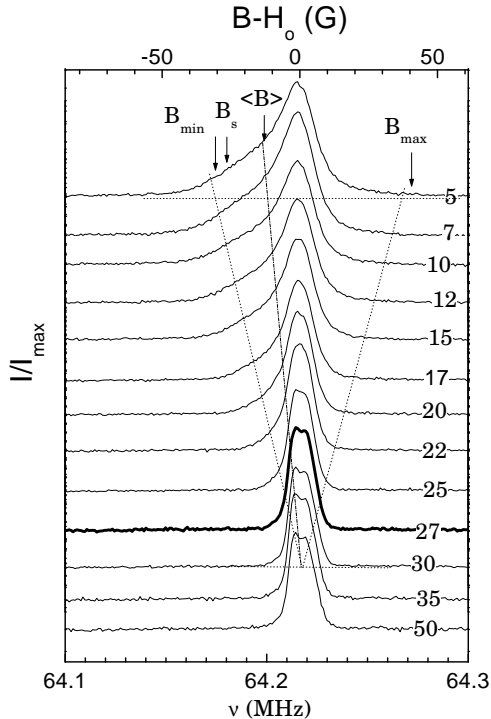


FIG. 2. ^{11}B NMR line shapes of the central transition in field 4.7 Tesla for $5\text{ K} \leq T \leq 50\text{ K}$. The dotted lines correspond to $\langle B \rangle$, $\langle B_{\max} \rangle$, and $\langle B_{\min} \rangle$.

Below T_{c2} ($\approx 27\text{ K}$ in 4.7 Tesla) the spectra start to broaden and under the irreversibility temperature an extra signal shows up as a pronounced shoulder in the low frequency part of the spectrum. It is worth noting that such an extra feature was not mentioned in previous NMR studies [8,21]. By further decreasing temperature the intensity of this shoulder increases and its location shifts to lower frequencies. This behavior is explicit to the magnetic field distribution in the mixed state, as implied by the dotted lines.

A significant part of the signal remains unshifted at the frequency of the normal state NMR signal. The unshifted part of the line shape may be explained if we consider a distribution of B_{c2} caused predominately by anisotropy and not by inhomogeneities, as the observed superconducting transition is extremely sharp. Assuming that the upper critical field depends on the angle of the c -axis in each crystallite then the angular dependence of the second critical field is given by $B_{c2}(\theta) = B_{c2}^{ab}(1 + (\gamma^2 - 1)\cos^2\theta)^{-1/2}$. This equation shows that only crystallites with $B_{c2}(\theta) > B_0$ would give a characteristic signal of a type-II superconductor in the mixed state. If for a part of the grains $B_0 > B_{c2}(\theta)$ then a NMR line shape would be observed, which is the sum of spectra coming from crystallites in the normal state and in the mixed state. Indeed the spectra under $B_0 = 4.7$

Tesla show an unshifted component which comes from the normal part of the sample, revealing the presence of strong anisotropy.

The two signal components are more clearly resolved in Figure 3, which shows ^{11}B NMR line shapes of the central transition in a magnetic field $B_0 = 2.35$ Tesla. In this field the low frequency shoulder becomes broader and shifts to lower frequencies in comparison to the spectra taken in 4.7 Tesla. This is expected if we consider that the magnetic field distribution in the vortex lattice becomes less dense and exhibits stronger field gradients in lower external magnetic fields. Since a significant part of the signal intensity remains unshifted, then it can be argued that for a part of the grains the B_{c2}^c must be lower than 2.35 Tesla. Considering that magnetization measurements give $B_{c2} \approx 14$ Tesla, and by assuming that $B_{c2}^{ab} > B_{c2}^c$ [11], [14] an anisotropy parameter $\gamma \geq 6$ is estimated.

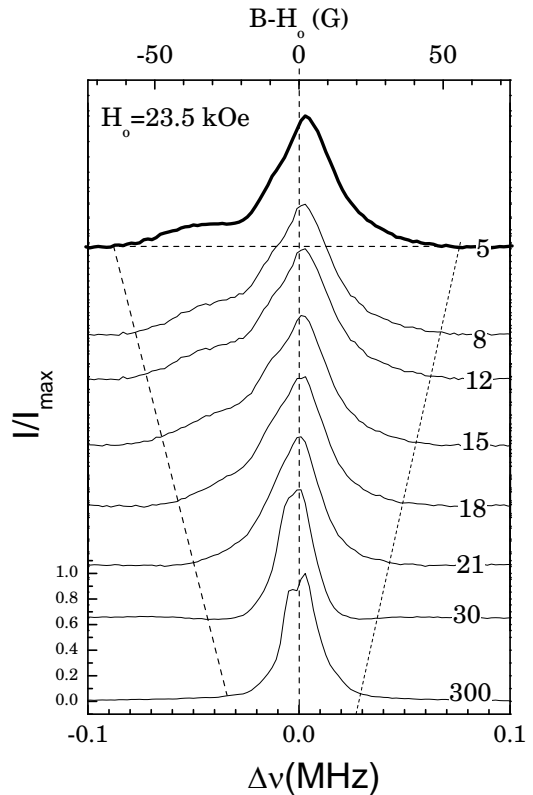


FIG. 3. ^{11}B NMR line shapes of the central transition in field 2.35 Tesla, as a function of temperature.

Following Ref. [18], a rough estimation of the singular points (at London limit $\lambda \gg \xi$) of the field distribution at $T = 5\text{ K}$ and $H = 4.7$ Tesla, gives: $B_{\max} - \langle B \rangle \approx 1.6 \times 0.551\Phi_0/4\pi\lambda^2 \approx 50$ Gauss, $B_{\min} - \langle B \rangle \approx -0.6 \times 0.551\Phi_0/4\pi\lambda^2 \approx -18$ Gauss and $B_s - \langle B \rangle \approx -0.5 \times 0.551\Phi_0/4\pi\lambda^2 \approx -15$ Gauss. In the above esti-

mations we used the experimental value of the magnetic induction at $T = 5$ K, $\langle B \rangle = 4\pi M_{rev} + H_o \approx -14 + H_o$ Gauss (see inset of Figure 1b) and $\lambda = 170$ nm.

The estimated values of B_{\max} , B_{\min} and B_s are in good agreement with the characteristic points (see arrows in Fig. 2) of the NMR spectrum at $T = 5$ K. *These results indicate that the low frequency shoulder of the NMR spectra is produced by the magnetic field distribution of the vortex lattice.*

The extension of the low field tail below the theoretical B_{\min} , and the slightly shifted broad maximum in the experimental magnetic field distribution might originate from small random perturbations by FL pinning or by structural defects in the FLL, which lead to smearing of the ideal field distribution. Deviation from the ideal distribution may be also produced by shearing of the FLL, which leads to splitting of the singularity at B_s and to the jump at B_{\min} , but leaves B_{\max} approximately unchanged [18]. Smearing from random shearing would dominate, if long-wavelength compression (flux density gradient) is not present, in particular for small or large B values, where the shear modulus $c_{66} \rightarrow 0$ for both $B/B_{c2} \rightarrow 0$ and $B/B_{c2} \rightarrow 1$. On the other hand, the magnetic field distribution is much more sensitive to fluctuations of the FLL density (random compression) than to shear deformations for $\langle B \rangle \gg 4\pi M$, if energetically favorable [23]. In such a case, even a small homogeneous compression of the FLL will shift rigidly the magnetic field distribution density [18], thus leading to smearing of all van Hove singularities. Finally, it should also be noted that in anisotropic superconductors the field distribution deviates from that of an isotropic hexagonal vortex lattice [24].

In conclusion, ^{11}B NMR line shape measurements on powder MgB_2 show up two NMR signal components for $T < T_{c2}$: one coming from the vortex lattice from grains in the mixed superconducting state, and another one from grains that are still in the normal state as their orientation in respect to the external magnetic field is such that $B_o > B_{c2}(\theta)$. Our measurements suggest a high anisotropy for the upper critical field with $\gamma \geq 6$, in agreement with recent CESR measurements [14]. This experimental result changes the balance in favor of anisotropic superconductivity in MgB_2 , and should be taken into consideration in theories trying to explain the superconducting state in this material.

* Permanent address, Department of Engineering Sciences, School of Engineering, University of Patras, 26110 Patras, Greece.

- [1] J. Nagamatsu *et al.*, Nature(London) **410**, 63 (2001).
- [2] T. H. Geballe, Science **293**, 223 (2001).
- [3] Y. Wang, T. Plackowski, and A. Junod, Physica (Amsterdam) **355C**, 179 (2001).
- [4] J. Kortus *et al.*, Phys. Rev. Lett. **86**, 4656 (2001).
- [5] S. L. Bud'ko *et al.*, Phys. Rev. Lett. **86**, 1877 (2001); Phys. Rev. B **63**, 220503 (2001).
- [6] G. Rubio-Bollinger, H. Suderow, and S. Vieira, cond-mat/0102242 (2001); G. Karapetrov *et al.*, cond-mat/0102312 (2001); A. Sharoni, I. Felner, and O. Millo, cond-mat/0102325 (2001).
- [7] H. Kotegawa *et al.*, cond-mat/0102334 (2001).
- [8] A. Gerashenko, K. Mikhalev, S. Verkhovskii, cond-mat/0102421 (2001).
- [9] H. Tou *et al.*, cond-mat/0103484 (2001).
- [10] S. L. Li *et al.*, cond-mat/0103032 (2001).
- [11] O. F. de Lima *et al.*, Phys. Rev. Lett. **86**, 5974 (2001).
- [12] M. Xu, H. Kitazawa, Y. Takano, J. Ye, K. Nishida, H. Abe, A. Matsushita and G. Kido, cond-mat/0105271 (2001).
- [13] S. Lee, H. Mori, T. Masui, Yu. Eltsev, A. Yamamoto and S. Tajima, cond-mat/0105545 (2001).
- [14] F. Simon *et al.*, Phys. Rev. Lett. **87**, 047002 (2001).
- [15] S. L. Bud'ko, V. G. Kogan and P. C. Canfield, cond-mat/0106577 (2001).
- [16] S. Patnaik *et al.*, Supercond. Sci. Technol. **14**, 315 (2001).
- [17] W. Fite, and A. G. Redfield, Phys. Rev. Lett. **17**, 381 (1966).
- [18] E. H. Brandt, Journal of Low Temp. Phys. **73**, 355 (1988); E. H. Brandt and A. Seeger, Advances in Physics **35**, 189 (1986); E. H. Brandt, Phys. Rev. Lett. **66**, 3213 (1991).
- [19] K.H. Lee *et al.*, Phys. Rev. B **62**, 123 (2000).
- [20] M. Pissas *et al.*, unpublished.
- [21] J. K. Jung *et al.*, Phys. Rev. B **64**, 012514 (2001).
- [22] M. H. Cohen and F. Reif, in Solid State Physics: Advances in Research and Applications, edited by F. Seitz and D. Turnbull (Academic Press, New York, 1957), Vol. 5.
- [23] Although we need higher energy to compress the FLL than to shear it, the field distribution will be dominated by random compressions when shear and compressional deformations will be of equal energy [18].
- [24] S. L. Thiemann, Z. Radovic, and V. G. Kogan, Phys. Rev. B **39**, 11406 (1989).